Supplementary Information

Chiroptical Properties of Bright Chiral Sulfur Quantum Dots with High-Yield Blue Luminescence

Karthika S Sunil[a]*, Hung-Ming Chen[b], Bramhaiah Kommula[c], Samir F. El-Mashtoly[a], Felix Otto[d], Marco Diegel[a], Christoph Krafft[a], Felix Herrmann-Westendorf[a], Nikita Vashistha[a], Benjamin Dietzek-Ivanšić[e], Hao-Wu Lin[b]*, Jer-Shing Huang [a,f,g,h,i]*

a. Leibniz Institute of Photonic Technology, Albert-Einstein-Straße 9, Jena 07745, Germany.
b. Department of Materials Science and Engineering, National Tsing Hua University, Hsinchu, Taiwan.
c. St. Joseph's University, Bengaluru-560027, Karnataka, India.
d. Institute of Solid-State Physics, Friedrich Schiller University Jena, Helmholtzweg 5, 07743 Jena, Germany.
e. Leibniz Institute for Surface Engineering, Permoserstraße 15, 04318 Leipzig, Germany.
f. Institute of Physical Chemistry, Friedrich-Schiller-Universität Jena, Jena 07743, Germany.
g. Abbe Center of Photonics, Friedrich-Schiller-Universität Jena, Jena 07743, Germany.
h. Research Center for Applied Sciences, Academia Sinica, Taipei 11529, Taiwan.
i. Department of Electrophysics, National Yang Ming Chiao Tung University, Hsinchu 30010, Taiwan.

TABLE OF CONTENTS

1. METHODS

Chemicals and materials

Milli-Q water was used throughout the reaction. All the chemicals were brought from Sigma-Aldrich. Ethylenediamine (≥99.5%), sulfur powder (100 mesh particle size), L-cysteine (≥98.5%), and D-cysteine (≥99%).

Synthesis of ethylenediamine-assisted sulfur dots (SDs)

Bulk sulfur (4 g) was dispersed in ethylenediamine (ED, 40 mL) and sonicated for 5 minutes to promote dissolution. The resulting mixture was transferred into a 25 mL Teflon-lined stainless-steel autoclave and heated at 170°C for 5 hours. After cooling to room temperature, the product was centrifuged at 7000 rpm for 10 minutes, and the process was repeated twice to ensure purification. The supernatant was concentrated using a rotary evaporator, followed by washing with ethanol. The purified material was dried at 50°C in an oven and further dried for 24 hours, yielding powdered SDs as shown in Figure S1.

The possible reaction mechanism is shown below:

Initially, the bulk sulfur dissolves in ED, leading to the formation of an alkylammonium polysulfide open-chain structure (eq.1). This intermediate subsequently reacts with H^+, generating zerovalent sulfur, which self-assembles and serves as the core of the SDs with an ED layer stabilizing the surface.

$$2H_2NCH_2CH_2NH_2 + S_x \rightarrow (H_2NCH_2CH_2NH_3^+)(H_2NCH_2CH_2NH - S_x^-) \quad \text{(eq.1)}$$

$$\left(H_2NCH_2CH_2NH_3\right)\left(H_2NCH_2CH_2NH - S_x^-\right) \overset{H^+}{\rightarrow} 2\left(H_2NCH_2CH_2NH_3^+\right) + S_x \quad \text{(eq.2)}$$

The H^+ required for the generation of zerovalent sulfur originates from H_2S, which forms as a byproduct of the reaction, as shown in equations 3 and 4:[1]

$$2H_2NCH_2CH_2NH_2 + S_x \rightarrow (H_2NCH_2CH_2NH)_2S_{x-1} + H_2S \quad \text{(eq.3)}$$

$$H_2NCH_2CH_2NH_2 + \frac{1}{4}S_8 \rightarrow H_2NCH_2CSNH_2 + H_2S$$ (eq.4)

Figure S1. Photograph of synthesized powdered SDs using the hydrothermal method.

Synthesis of L-cysteine and D-cysteine SDs (L- and D-SDs)

Chiral SDs (cSDs) were synthesized via the thermal polymerization method. This method was utilized to make the carbon dots chiral by Wang et. *al*.[2] in 2022. Powdered SDs (50 mg) were dispersed in 3 mL of water and stirred for 10 minutes. L- or D-cysteine (50 mg) was then added to the mixture, and the reaction mixture was maintained at 180°C for 1 hour under continuous stirring. Following the reaction, the solution was cooled to room temperature and centrifuged to isolate the purified chiral L/D-SDs.

2. CHARACTERIZATIONS

Transmission electron microscopy (TEM)

The diluted samples were drop-casted in a carbon grid and dried before the measurements. TEM images were captured using the instrument JEOL NEOARM 200 F. The achiral SDs showed an average diameter of ~4.3 nm and a lattice fringe of 0.22 nm, as shown in Figure S2.

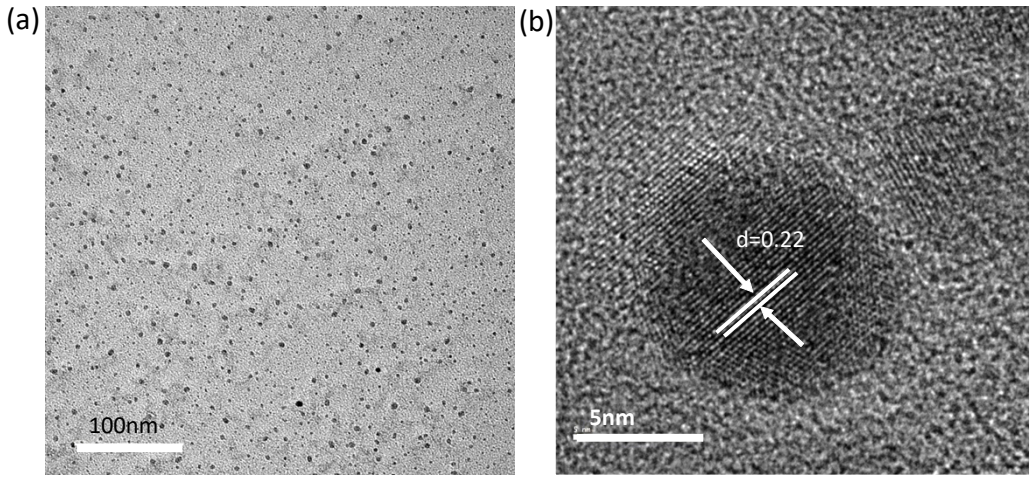

Figure S2 TEM image of SDs (a) TEM of achiral SDs with an average diameter of ~ 4.3nm (b) High-resolution TEM image of achiral SDs with a lattice fringe of ~0.22nm.

X-ray photoelectron spectroscopy (XPS)

The samples were drop-casted on a silicon wafer, dried in an oven, and vacuumed to evaporate the moisture content in the sample. The XPS analysis of the film was performed with an XR 50 M X-ray source coupled with a FOCUS 500 monochromator (manufactured by SPECS Surface Nano Analysis GmbH, Berlin, Germany) utilizing Al Kα radiation (1486.7 eV) under normal emission at ambient temperature. Detection of photoelectrons was achieved through a PHOIBOS 150 hemispherical analyzer, which was equipped with a delay line detector (model 3D DLD4040-150). Calibration of the binding energy for the samples was done using an energy C_{1s} peak at 284.8 eV. The overall XPS spectrum, and a comparison of high-resolution XPS spectra between the achiral SDs and cSDs are depicted in Figure S3.

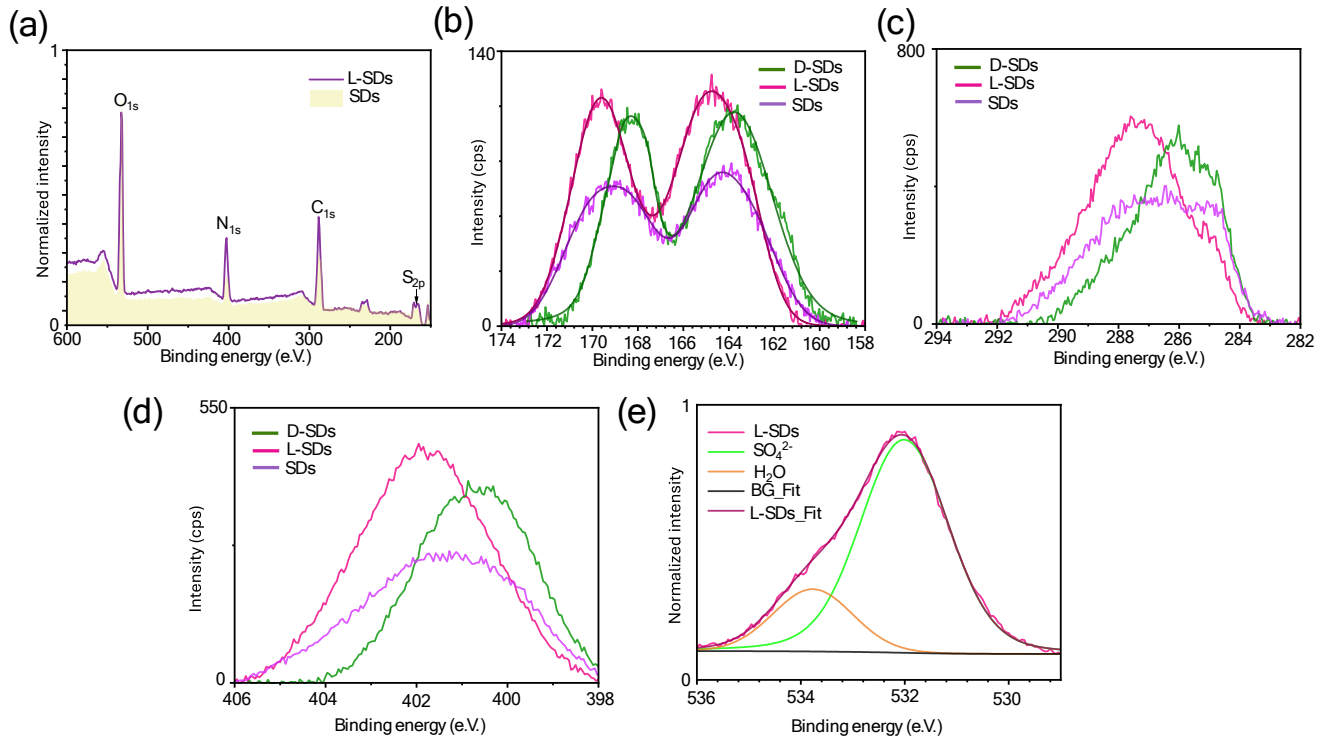

Figure S3 X-ray photoelectron spectroscopy (XPS) analysis of achiral SDs and cSDs. (a) Overall XPS spectra of both L-SDs (magenta solid line), achiral SDs (light yellow shaded region) show O_{1s}, N_{1s}, C_{1s}, and S_{2p} peaks. High-resolution XPS of achiral SDs (purple), L-SDs (magenta), and D-SDs (green) of (b) S_{2p} (c) C_{1s} (d) N_{1s} show the spectral shift between L- and D-SDs compared with that of achiral SDs. (e) High-resolution O1s XPS spectra of L-SDs (magenta) showing sulphate (lime) and water peak (orange).

Infrared spectroscopy (IR)

IR spectra of achiral SDs and cSDs were acquired using a Cary 670 FTIR spectrometer (Agilent, USA). For this purpose, an ATR accessory equipped with a ZnSe crystal featuring triple reflection (Miracle, Pike Technologies, USA) was utilized. Spectra were recorded in the 900–4000 cm^{-1} range using a DTGS detector. Approximately 5–10 µL of each liquid sample was applied directly to the ATR crystal. A spectrum of each compound was recorded after evaporation of the water by averaging eight scans collected per measurement.

Figure S4 Infrared spectra of D-SDs.

Raman spectroscopy

Raman spectroscopic measurements were acquired using a WITec alpha 300R confocal Raman microscope (Ulm, Germany). A diode laser of 785 nm (Toptica Photonics AG, Munich, Germany) was used as the excitation source with an output power of approximately 300 mW. The laser radiation was coupled into a Zeiss microscope through a wavelength-specific single-mode optical fiber. The laser beam focused on the sample through a 10x objective (Olympus). Raman back-scattered light was collected through the same microscopic objective and passed through a holographic edge filter onto a multimode fibre (100 µm diameter) and guided to a spectrometer (UHTS300, WITec, Germany) entrance. The collected light was dispersed by a blazed 600/mm grating at 750 nm. Raman spectra were detected by a back-illuminated deep-depletion charge-coupled device (CCD) camera operating at −60°C. The incident laser power on the sample was 20 mW with an integration time of 1 second and 20 accumulations.

Figure S5 shows the Raman spectra of the cSDs and achiral SDs compared with that of pure L-cysteine. The peaks at ~470 cm^{-1} and ~981 cm^{-1} correspond to elemental sulfur in S_8 and the υ_1 modes of sulfate groups, respectively, further supporting the formation of SDs with sulfur and sulfur oxides, which is in agreement with the XPS analysis.[3, 4] The presence of the -S-S- peak can be seen around ~547cm^{-1} for all the SD samples and is absent in pure cysteine,[5] and the -C–S- stretching can be seen around 666 cm^{-1}.[5] All these peaks, along with those mentioned in the main manuscript, represent the successful formation of cSDs.

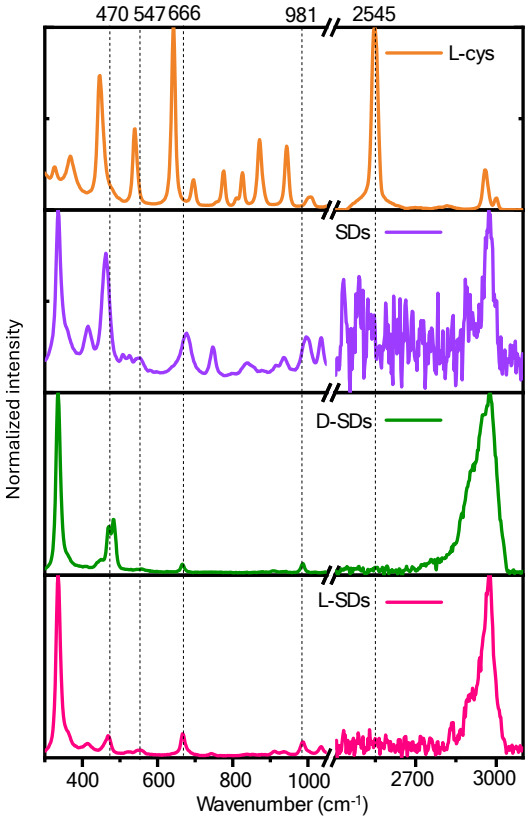

Figure S5 Raman spectra of cSDs (L-SDs: magenta, D-SDs: green) and achiral SDs (purple) compared with that of the L-cysteine (orange).

Overall, from IR and Raman analysis, the possible equation for the formation of chiral SDs can be written as,

$$2\left(H_2NCH_2CH_2NH_3^+\right) + S_x + HSCH_2CH(NH_2)COOH \rightarrow 2\left(H_2NCH_2CH_2NH_3^+\right) + S_x + (S)^-CH_2CH(NH_2)COO^-$$

(eq.5)

Photoluminescence quantum yield (PLQY) measurements

The absolute PLQY of the samples was determined using the FLS 980 instrument from Edinburgh Instruments with an integrated sphere. The absorption value at the excitation wavelength was fixed to 0.1 OD to reduce reabsorption. The PLQY (Φ) is defined as,

$$\Phi = \frac{number\ of\ emitted\ photons}{number\ of\ absorbed\ photons} \quad \text{(eq.6)}$$

In this approach, PLQY is measured without using a reference sample, unlike the conventional relative method. Instead, an integrating sphere is used to directly determine the amount of light absorbed by the sample, calculated by subtracting the transmitted excitation light (measured using a blank, such as water) and the amount

of light emitted by the sample, obtained from the integrated emission spectrum.[6] A comparison chart for the PLQY enhancement for achiral SDs after coating them with cysteine is given below.

Table 1 The enhancement of PLQY for L-SDs and D-SDs is compared with that of achiral SDs.

	L-SDs	D-SDs	Achiral SDs
340 nm excitation	86.6%	81.6%	79.3%
260 nm excitation 270 nm excitation	20.4%	20.6%	 3.4%

Table 3: PLQY stability test conducted for the chiral samples L-SDs and D-SDs by measuring PLQY before and after 2 weeks.

340 nm excitation	Day (0)	Day (14)
L-SDs	88.7 %	89.2%
D-SDs	86.3 %	82.2 %

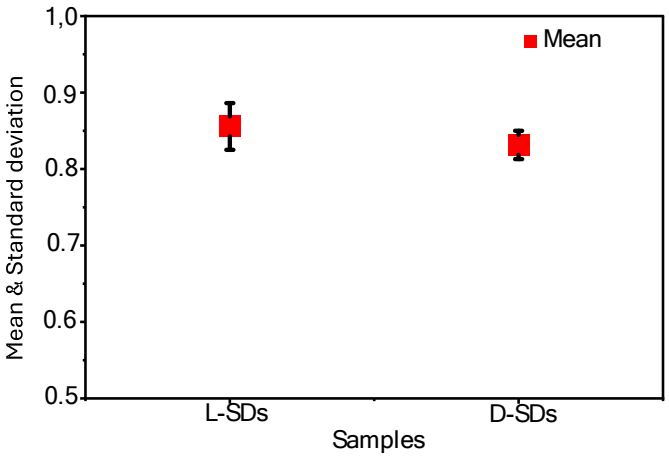

Figure S6 Mean and standard deviation plot of the chiral samples L-SDs and D-SDs having PLQY > 80% with standard deviation less than 0.04.

Lifetime measurements

Fluorescence lifetime measurements were performed using a time-correlated single-photon counting (TCSPC) system (PicoQuant Flu Time 200). Samples were excited at 375 nm with a picosecond diode laser (LDH-375, PicoQuant), and the emission decay was recorded at the photoluminescence maximum of each sample.

Circular dichroism (CD)

The samples were diluted in water and filled in a 10 mm pathlength cuvette and measured in the JASCO J-810 spectropolarimeter. The CD spectra of pure L- and D-cysteine shown in Figure S6 display a single peak at 200 nm, indicating that any peaks observed in the cSDs beyond 200 nm arise from induced chirality rather than the intrinsic chirality of cysteine itself.

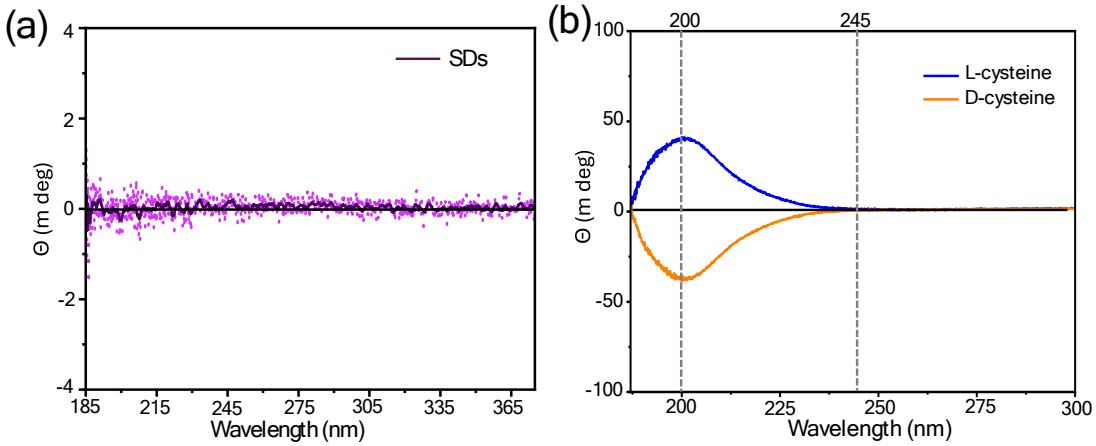

Figure S7 Circular dichroism spectra of (a) achiral SDs, raw data are plotted as purple dots, and (b) pure ligands; L-cysteine (blue) and D-cysteine (orange). The zero baseline is indicated by a black horizontal line in panels (a) and (b).

3. CIRCULAR POLARIZED LUMINESCENCE (CPL)

The CPL measurement is carried out by the optical setup shown in the schematic diagram in Figure S7a. Initially, the samples in a cuvette were excited with a 375 nm laser. The emission from the sample comprises both left- and right-handed circularly polarized light (l- and r-CPL) components, which are then passed through a quarter-wave plate (QWP), converting the circularly polarized signal into a linearly polarized one. A 50:50 beam splitter was placed after the QWP, which resulted in two beams that were then passed through linear polarizers with perpendicular transmission axes and were collected using a Y-shaped optical fiber (Figure S7a). The left- and right-handed CPL spectra were measured simultaneously using a spectrometer coupled to a CCD camera, as illustrated in Figure S7a. During the measurements, the linear polarizers remained fixed, while the quarter-wave plate was switched between 0° and 90° to change the detected polarization handedness between the two channels. By averaging the signals from both channels, systematic errors like beam path asymmetry were effectively minimized.

Figure S8 (a) Schematic diagram for the home-built optical setup for circular polarized luminescence measurements (CPL). (b) The CPL dissymmetric factor plot for achiral SDs showing zero CPL, the raw data are plotted as purple dots.

The dissymmetric factor is calculated as the difference between the fluorescence intensities of l- and r-CPL components divided by their average, as shown in Eq. 7.

$$g_{FDCD} = \frac{2(F_{L\_} F_R)}{(F_L + F_{R)}} \qquad \text{(eq. 7)}$$

Where F_L and F_R are the fluorescence intensities of l- and r-CPL components. The difference between them is plotted below.

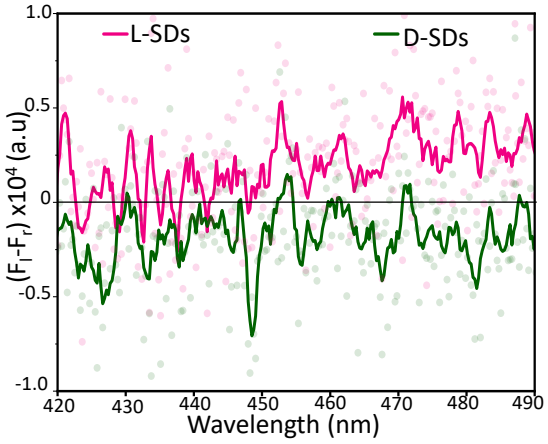

Figure S9 Fluorescence intensity difference (F_L - F_R) between l- and r-CPL components of emission is plotted against wavelength of emission.

4. FLUORESCENCE-DETECTED CIRCULAR DICHORISM (FDCD)

A modified Jasco FP-8300 CD spectrometer equipped with an FDCD accessory is used to measure FDCD.[7] A long-pass filter and lenses were arranged at a 90° angle relative to the excitation beam, which enabled the collected fluorescence to be directed to an auxiliary detector (e.g., a photomultiplier tube). In FDCD spectroscopy, the DC voltage varies while the HT voltage on the photomultiplier tube is held constant, unlike the CD. The differential circularly polarized fluorescence excitation (ΔF), which shows the fluorescence intensity difference upon left- and right-circularly polarized excitation (F_l and F_r), is obtained from FDCD spectroscopy (eq. 8). The DF value from the spectroscope is concentration-dependent, hence to get a concentration-independent parameter, DF is normalized by the total fluorescence intensity (F_l+ F_r), corresponding to the DC component (eq. 9). This normalized parameter is called the g_{FDCD} value. It can be considered as the fluorescence-based analog of the molar circular dichroism, although derived through a more complex mathematical method.

$$\Delta F = F_l - F_r \qquad \text{(eq.8)}$$

$$g_{FDCD} = \frac{\Delta F}{(F_l + F_{r)}} \qquad \text{(eq.9)}$$

where F_l and F_r are the fluorescence intensities at left- and right-handed circular polarized excitation, respectively. The ΔF versus excitation wavelength is plotted below;

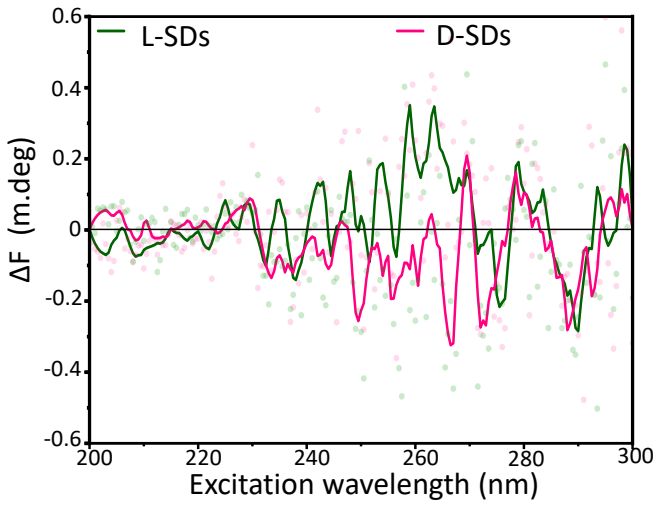

Figure S10 The difference in fluorescence intensities when excited with l-CPL and r-CPL (ΔF) is plotted as a function of excitation wavelength.

REFERENCE

Cited at the end of the main manuscript